Compositional differences between preterm milk of different gestational ages with the term milk: a comparative lipidomic study by LC-MS/MS

Ying-chun Zhao
Children's Hospital of Shanghai
Ying Zhang
Children's Hospital of Fudan University
Chun-xue Liu
Children's Hospital of Fudan University
Dong-yong Yan
Children's Hospital of Fudan University
Ping Dong (dongping@fudan.edu.cn)
Children's Hospital of Fudan University

Research

Keywords: human milk, lipidomic, LC-MS/MS, very preterm, extremely preterm, infants

Posted Date: September 8th, 2021

DOI: https://doi.org/10.21203/rs.3.rs-861207/v1

Abstract

Background

Studies are beginning to emerge on the important biological effects of the milk lipids exerted on the recipient infant, especially on the premature infants. The aim of this study was to comprehensively describe lipidomic differences between preterm milk of different gestational ages with the term milk over the course of lactation.

Methods

Breast milk samples were collected from 88 mothers giving birth prematurely and 39 mothers delivering at full-term (FT). Lipid profiles were assessed using an LC-MS/MS metabolomics strategy. Orthogonal partial least-squares discriminant analysis (OPLS-DA) and pathway analysis were subsequently performed.

Results

The OPLS-DA score plots significantly distinguished the lipids in preterm milk of different gestation ages from their counterparts in term milk. The concentrations of 10 out of 43 lipid subclasses were found to be persistently higher in preterm compared to term milk over the course of lactation; the diacylglycerol (DAG) and a bioactive subclass fatty acid ester of hydroxyl fatty acid (FAHFA) contributed the most to the differences. In terms of individual lipid species, the ten highest substances found in very preterm (VPT) colostrum compared to FT colostrum mainly come from the phosphatidylethanolamine class and the DAG species. Lipid species from the free fatty acid and FAHFA classes were significantly higher in either extremely preterm (EPT) or VPT mature milk (variable importance in projection > 1, $P < 0.0001$ for all). The differential lipids between each preterm group and its term counterpart were predicted to be mainly involved in six metabolic pathways, including glycerophospholipid metabolism, glycosylphosphatidylinositol (GPI)-anchor biosynthesis, linoleic acid metabolism, alpha-Linolenic acid metabolism, arachidonic acid metabolism and glycerolipid metabolism.

Conclusions

The lipids in preterm and term milk showed substantial differences, which may be critical for postnatal growth, as well as the neural and immune development of newborns, especially EPT and VPT.

Introduction

Premature infants are high-risk groups for growth and neurodevelopmental retardation, as well as infectious diseases, and these are the main causes of death for children under 5 years old. With the continuous progress of perinatal medicine and intensive care technology, increasing numbers of premature infants with short gestational ages and low birth weights are surviving. How to ensure the appropriate growth of premature infants, prevent all kinds of infectious and non-infectious diseases, and improve the prognosis of nerve development while improving survival rate, are all important issues of global concern, and are essential to improving the quality of life and population of children. The World Health Organization (WHO) defines gestational age (GA) ≥ 28 weeks but < 32 weeks as very preterm (VPT), while GA < 28 weeks is defined as extremely preterm (EPT). Although VPT and EPT account for only 2% of all live births and about 16% of all premature infants, the mortality, disease incidence and long-term adverse prognosis of VPT and EPT are much higher than those of moderate preterm (MPT) infants, with a GA ≥ 32 and < 37 weeks [1, 2].

Human milk (HM) is very important for infants, as it provides all the energy and nutrients normal infants require within 6 months. Breastfeeding has multiple benefits for premature infants, such as improved immunity, decreased morbidity and mortality associated with necrotizing enterocolitis, better neurodevelopmental outcomes and improved long-term health outcomes [3–6]. Lipids are one of the most important energy substances in HM, and provide essential vitamins, polyunsaturated fatty acids, complex lipids, and bioactive components to the recipient infants. The biological effects of the lipids provided to breastfeeding infants, for example, on gastrointestinal maturation, lipid and lipoprotein metabolism, membrane composition and function, neurodevelopment and immune function, have also been recognized [7, 8]. Furthermore, the lipid profile of HM impacts early growth in preterm infants [9].

Days postpartum (lactation stage), GA and maternal diet are factors known to influence HM content [10]. Many researchers have already performed dozens of valuable studies on the specific lipid classes in HM, such as triacylglycerol (TAGs) [11, 12] or phospholipids (PLs) [13, 14]. With present-day “omics” techniques, a comprehensive and quantitative analysis of HM lipid composition has become possible. Liquid

chromatography tandem–mass spectrometry (LC-MS/MS) is extensively applied in identifying untargeted lipid profiles, due to its high resolution and precision [15]. Both Sokol, E. et al [16] and Hewelt-Belka, W. et al [17] used the comparative LC-MS/MS strategy to investigate the lipidomic differences between HM and formula milk (FM), and found that the lipid composition of FM deviates significantly from that of HM. They also observed significant differences between colostrum and HM collected at other lactation stages.

Metabolomic studies on preterm and full-term (FT) milk have revealed significant differences in the presence of metabolites important for infant development, such as phosphocholine, lysine and glutamine [18]. However, lipidomic studies using LC-MS/MS to compare preterm and FT milk over the course of lactation are still scarce. Ingvordsen Lindahl, I.E. et al. [19] focused on the PL profile of preterm milk (mean GA 30.8 ± 3.4 weeks), and found that both GA and age postpartum affected the 31 PL species found in HM during the first 15 weeks postpartum. Significantly higher concentrations of phosphatidylcholine (PC), sphingomyelin (SM) and total PL were found in preterm milk throughout lactation. Xu, L et al. [20] recently collected six MPT and six FT colostrum samples from healthy breastfeeding mothers, and found that phosphatidylethanolamine (PE) and PC were robustly increased, while diacylglycerol (DAG) and ceramide were markedly decreased, in MPT colostrum. Besides these two studies, data concerning lipid composition differences between preterm and FT milk are remarkably scarce. This knowledge gap must be filled in order to further determine the impacts of these differential lipids on infant growth and development, as well as to provide suitable nutrition for premature infants, particularly EPT and VPT.

In the current study, we conducted an LC-MS/MS-based comparative lipidomic analysis of HM from different GA, using a relatively large sample. Lipid profile differences were assessed by: (i) comparison of VPT and MPT colostrum with its FT counterparts; (ii) comparison of EPT, VPT and MPT mature milk with its FT counterparts. As far as we know, this study is the first to comprehensively describe differences between preterm and term milk lipidomes over the course of lactation.

Materials And Methods

Ethical Approval

Informed consent was obtained from all subjects involved in the study. Ethical approval for this study was granted by the Ethics Committee of the Children's Hospital of Fudan University (Children's Hospital of Fudan University Ethics Protocol 2019–087).

Milk Sample Collection

Preterm milk samples of known GA and lactational stage were collected from non-smoking, non-diabetic mothers in the neonatal intensive care unit of the Children's Hospital of Shanghai (Shanghai, China). Colostrum (<5 postpartum days, n=20 for VPT, n=20 for MPT) and mature milk samples (4 weeks postpartum, n=11 for EPT, n=23 for VPT and n=21 for MPT) spanning 24/0 weeks to 36/4 weeks of gestation were collected by 88 mothers with preterm (delivered before the 37th week of gestation) infants. The mean age of the mothers was 31.5 years, mean gestational age was 30.25 weeks and mean infant weight at birth was 1470 grams (Table 1). It is difficult to collect sufficient colostrum from EPT mothers, thus the corresponding samples were not collected. FT milk samples were obtained from the Women's Hospital of Nanjing Medical University, Nanjing Maternity and Child Health Care Hospital (Nanjing, China). Colostrum (n=30) and mature milk samples (n=25) were donated by 39 mothers who had delivered healthy and term (delivered after the 37th week of gestation) infants. Preterm and term samples were kept at −80 °C until analysis.

Metabolites Extraction

As previous studies have described [21, 22], 100 μL of sample was transferred to an EP tube, and mixed with 480 μL of extract solution (MTBE:methanol = 5:1) containing internal standard. After 30 s of vortexing, the samples were sonicated for 10 min in an ice-water bath. Then, the samples were incubated at -40 ℃ for 1 h and centrifuged at 3000 rpm for 15 min at 4 ℃. A total of 350 μL of supernatant was transferred to a fresh tube and dried in a vacuum concentrator at 37 ℃. Then, the dried samples were reconstituted in 100 μL of 50% methanol in dichloromethane by sonication for 10 min in an ice-water bath. The solution was then centrifuged at 13000 rpm for 15 min at 4 ℃, and 90 μL of supernatant was transferred to a fresh glass vial for LC-MS/MS analysis. The quality control (QC) sample was prepared by mixing an equal aliquot of the supernatants from all of the samples.

LC-MS/MS Analysis

LC-MS/MS analyses were performed using an UHPLC system (1290, Agilent Technologies), equipped with a Kinetex C18 column (2.1 × 100 mm, 1.7 μm, Phenomen). The mobile phase A consisted of 40% water, 60% acetonitrile, and 10 mmol/L ammonium formate. The mobile phase B consisted of 10% acetonitrile and 90% isopropanol, which was mixed with 50 mL of ammonium formate, added at 10 mmol/L for every 1000 mL of mixed solvent. The analysis was performed with the following elution gradient: 0~12.0 min, 40~100% B; 12.0~13.5 min, 100% B; 13.5~13.7 min, 100~40% B; 13.7~18.0 min, 40% B. The column temperature was 55 ℃. The auto-sampler temperature was 4 ℃,

and the injection volume was 2 μL (pos) or 4 μL (neg) [21]. The QE mass spectrometer was used as it can acquire MS/MS spectra in the data-dependent acquisition (DDA) mode under the control of the acquisition software (Xcalibur 4.0.27, Thermo). In this mode, the acquisition software continuously evaluates the full-scan MS spectrum. The ESI source conditions were as follows: sheath gas flow rate 30 Arb, Aux gas flow rate 10 Arb, capillary temperature 320 ℃ (positive) and 300 ℃ (negative), full MS resolution 70000, MS/MS resolution 17500, collision energy 15/30/45 in NCE mode, spray voltage 5 kV (positive) or −4.5 kV (negative) [23, 24].

Data preprocessing and annotation

The raw data files were converted to the mzXML format using the "msconvert" program from ProteoWizard. Peak detection was first applied to the MS1 data. The CentWave algorithm in XCMS was used for peak detection in the MS/MS spectrum, while lipid identification was achieved through spectral matching using the LipidBlast library. We applied orthogonal partial least-squares discriminant analysis (OPLS-DA) to the unit variance-scaled spectral data so as to visualize the differences between preterm and term milk. The coefficient loading plots and variable importance in projection (VIP) of the OPLS-DA model were employed for identifying the spectral variables related to sample dissolution. The VIP scores ranked the components according to their role in the observed separation [24, 25]. Statistical distinctness was established using Student's t-test, with $P < 0.05$ signifying significance. We conducted pathway assessments in MetaboAnalyst (http://www.metaboanalyst.ca/).

Results

Multivariate statistical analysis of lipids

Based on the OPLS-DA, the score scatter plot indicates a distinct separation between each preterm group and its term counterpart. The sample is basically within the 95% confidence interval (Hotelling's T-squared ellipse) (Figures 1-5). The R^2Y and Q^2Y values in the OPLS-DA model were all > 0.5 (in the comparison of VPT colostrum and FT colostrum, $R^2Y = 0.829$ and $Q^2 = 0.665$ in the negative ionization mode, and $R^2Y = 0.817$ and $Q^2 = 0.644$ in the positive ionization mode; in the comparison of MPT colostrum and FT colostrum, $R^2Y = 0.88$ and $Q^2 = 0.788$ in the negative ionization mode, and $R^2Y = 0.851$ and $Q^2 = 0.756$ in the positive ionization mode; in the comparison of EPT mature milk and FT mature milk, $R^2Y = 0.822$ and $Q^2 = 0.747$ in the negative ionization mode, and $R^2Y = 0.776$ and $Q^2 = 0.733$ in the positive ionization mode; in the comparison of VPT mature milk and FT mature milk, $R^2Y = 0.771$ and $Q^2 = 0.684$ in the negative ionization mode, and $R^2Y = 0.718$ and $Q^2 = 0.597$ in the positive ionization mode; in the comparison of MPT mature milk and FT mature milk, $R^2Y = 0.804$ and $Q^2 = 0.713$ in the negative ionization mode, and $R^2Y = 0.788$ and $Q^2 = 0.758$ in the positive ionization mode), implying that the OPLS-DA model was well-determined. These OPLS-DA models were further validated using permutation tests of training sets of 100 times. The R^2Y and Q^2 values were the greatest in the current sample clustering approach, and the longitudinal intercept of the Q^2 regression line is less than zero. Therefore, the original model has good robustness, without overfitting (Figures 1-5).

Lipid profiling differences between preterm and term HM

Based on the results of the LC-MS/MS analysis, more than nine thousand lipid substances were found in the HM sample. In general, 113-272 lipids (VIP > 1, $p < 0.05$) were remarkably different when comparing each preterm group with its term counterpart. All of the markedly different lipids are shown in Additional file 1: Table S1-S2. For each group, we calculated the Euclidean distance matrix for the quantitative values of differential lipids, and clustered the differential lipids using the complete linkage method, which we then displayed as a heatmap (see Additional file 2: Figures S1-S10). The top 10 most noticeably up-modulated and down-modulated lipids in each preterm arm in positive ion mode and negative ion mode respectively were listed in Additional file 3: Table S3-S6.

As previously mentioned, we were particularly interested in the unique characteristics of EPT and VPT milk in terms of lipid composition. After eliminating the lipids identified in both the positive, as well as the negative ion mode repeatedly, we found that the top 10 substances that were higher in the VPT colostrum than in the FT colostrum were mostly from the PE class (18:1/22:1, 18:1/20:1, 14:1/26:4 and 16:0/16:0) and the DAG species (12:0/22:5, 16:0/22:6 and 14:1/18:1) (Table 2). In terms of mature milk, lipids from free fatty acid (FA) (18:1, 16:2, 17:3 and 19:2) and a bioactive class fatty acid ester of hydroxyl fatty acid (FAHFA) (16:1/22:4, 22:3/22:4, 2:0/17:2 and 20:2/20:1) constituted the 10 most upregulated substances in the EPT group, as compared with their FT counterparts (Table 3); similarly, lipids from FA (16:2, 17:3 and 18:1) and FAHFA (18:2/14:1, 16:1/22:4, 20:3/22:5, 12:0/18:2 and 18:1/18:2) constituted the 10 most upregulated substance in the VPT group, compared with their FT counterparts (Table 4).

The differences in the comparative proportion of identified lipid species

The differences in the proportions of identified lipid species were used to reveal their composition and distribution. After combining the positive and negative ionization modes, among the 43 subclasses of lipids, we found that the concentrations of acylcarnitine (ACar), ceramide alpha-hydroxy fatty acid-phytospingosine (Cer/AP), ceramide alpha-hydroxy fatty acid-sphingosine (Cer/AS), DAG, Diacylglyceryl trimethylhomoserine (DGTS), FA, FAHFA, lysophosphatidylethanolamine (LPE), monoacylglycerol (MAG), PC and PE were significantly higher in both the VPT and MPT colostrum than in the FT counterparts (Figures 6). The differences in mature milk are generally consistent with those in colostrum, but the level of DGTS did not increase significantly in each premature group compared with the FT counterparts (Figures 7). The two most significantly upregulated lipid clusters in the preterm arm were FAHFA and DAG, in both colostrum and mature milk (Figures 6 and 7).

The Metabolomic Pathways of the Differential Lipids Between the Term and Preterm Milk

Pathway analysis was performed using MetaboAnalyst to explore the potential functions of the significantly different lipids. These lipids were predicted to be involved in six metabolic pathways, including glycerophospholipid metabolism, glycosylphosphatidylinositol (GPI)-anchor biosynthesis, linoleic acid metabolism, alpha-Linolenic acid metabolism, arachidonic acid metabolism and glycerolipid metabolism (Figure 8).

Discussion

Advances in metabolomics and lipidomics using LC-MS/MS have enabled the accurate quantification of complex lipid molecules in milk, as well as in very small amount of infant serum or plasma [26-29]. Such lipidomic measurements can provide markers for tissue composition [30], and have been proven to be related to many important clinical endpoint events in children and adults [31-33]. Therefore, using these sophisticated and detailed analytical methods in conjunction with appropriate bioinformatics strategies should provide a better understanding of the physiological role of complex lipids in early life.

According to our LC-MS/MS results, in terms of the total contents of major lipid subsets, the concentrations of 10 out of the 43 lipid subclasses were found to be persistently higher in preterm milk compared to term milk over the course of lactation, with the FAHFA and DAG classes contributing the greatest differences. The difference between preterm milk of different GA stages and term milk is relatively consistent; in other words, the composition of preterm milk did not visibly resemble that of term milk as GA increased. In terms of individual lipid species, differential lipids (VIP > 1, $p < 0.05$) between preterm and term milk began to show discrepancies with increasing GA of the neonate and the progression of lactation. As mentioned in the background section, we paid special attention to EPT and VPT milk. Interestingly, compared with their FT counterparts, several PLs from the PE class (18:1/22:1, 18:1/20:1, 14:1/26:4 and 16:0/16:0) and the DAG species (12:0/22:5, 16:0/22:6 and 14:1/18:1) in VPT colostrum were significantly higher. In mature milk, FA and FAHFA lipids comprised the 10 most upregulated substances in both the EPT and VPT groups ($P<0.0001$ for all).

DAG is one of the primary lipid subpopulations in living systems, and acts as a second messenger in multicellular activities. It has been reported that DAG can accelerate the β-oxidation of fatty acids and affect the expression of genes related to lipid metabolism, thereby reducing TAG levels in serum and liver [34, 35]. In our current study, we found the total concentrations of DAG to be markedly increased in both preterm colostrum and mature milk, and several individual DAG species, such as DAG 12:0/22:5, 16:0/22:6 and 14:1/18:1 were significantly elevated in the VPT colostrum. The high levels of DAG species in preterm human milk may be linked to enhanced long-term health outcomes; for instance, reduced obesity, diabetes, and cardiovascular disease. Interestingly, Xu, L et al. [20] reported that DAG levels were significantly reduced in the colostrum of mothers who gave birth prematurely. Discrepancies between the present study and that of Xu, L et al. might stem from the significantly smaller sample size (n= 6, in both the preterm group and term groups) and greater GA of premature delivery (32–36 weeks) in the latter. More research is needed to validate our findings.

FAHFAs have come to be recognized as one of the bioactive lipids present in the HM with anti-inflammatory, anti-diabetic effects; they enhance glucose tolerance and the secretion of insulin and glucagon-like peptide 1 (GLP-1) while reducing inflammation [36-39]. Lee, J. et al. [40] also reported the role of FAHFAs in the gut, regulating both innate and adaptive immune responses in a model of colitis. So far, FAHFAs have only been detected in the serum and adipose tissue of mice and humans [36], and adipose tissue represents a major site for FAHFAs synthesis [36, 37]. Brezinova M et al. [41] performed a lipidomic analysis of milk samples obtained from lean and obese mothers, and compared the PAHSA (an FAHFA species containing palmitic acid) levels of these groups. They found, for the first time, that lipids from the FAHFA family exist in human colostrum/transient milk, and that the concentration of FAHFA in HM was negatively correlated with maternal weight. As can be seen from the above, FAHFAs hold great biological significance, but little research has been done on FAHFAs in HM, except the above. For the first time, we found that the levels of FAHFAs in preterm HM at different GAs were significantly higher than in term HM, with the levels of several FAHFA species (16:1/22:4, 22:3/22:4, 2:0/17:2, 20:2/20:1, 18:2/14:1, 16:1/22:4, 20:3/22:5, 12:0/18:2 and 18:1/18:2) remarkably higher in either EPT or VPT mature milk compared with their FT counterparts. Our findings may indicate that FAHFAs

play an important role in improving the metabolism and promoting the intestinal maturation of premature infants. More maternal–child cohort studies and animal experiments will be needed to further explore the role and the mechanism of action of FAHFAs in HM.

PLs are a class of lipids with important biological functions, despite only accounting for 1% of total milk lipids [42]. They are involved in the digestion, absorption and transport of TAG, making up the milk fat globule membrane and providing important bioactive components, such as choline, and the long-chain polyunsaturated fatty acids fatty acids (LC-PUFAs) docosahexaenoic acid (DHA) and arachidonic acid (AA), which are crucial for the neural and visual development and growth of the neonate [43-46]. The glycerophospholipids (GPL) PC and PE, and the sphingolipid (SL) SM, are the three major PL classes found in HM. So far, omics has rarely been used to thoroughly study the PLs in both preterm and term milk from different gestation ages and lactation stages.

Here, we show that the total concentration of PE was increased in both preterm colostrum and mature milk, and several individual PE species, such as PE 18:1/22:1, 18:1/20:1, 14:1/26:4 and 16:0/16:0, were significantly elevated in the VPT colostrum. PE, also known as cephalin, is an important part of the nerve cell membrane. It regulates all the metabolic activities of nerve cells and affects a series of important functions of nervous tissue, such as cell permeability, myelin formation and mitochondrial operation [7]. Our results highlight the important role that the PE in HM plays in the early nervous system development of premature infants. Furthermore, LC-PUFAs are often found as FA moieties of PE, and contribute to the neurological as well as visual development of the neonate [47,48]. The transport of LC-PUFA from mother to infant mainly occurs through the placenta in late pregnancy. The dramatically higher content of PE observed in both preterm colostrum and mature milk in our findings suggests that the PE in HM may be an important channel through which premature infants with low GAs can obtain sufficient LC-PUFA through breastfeeding. Furthermore, in the present study, the observed differences in PE between preterm and term colostrum were almost equally prominent in mature milk, which diverges from the observations of Ingvordsen Lindahl, I.E. [19], wherein the effects of gestation subsided in mature milk. Discrepancy might be influenced by the sample preparation process, especially the addition of different internal standards prior to lipid extraction. More homogenization and standardized HM lipidomic studies starting from sample collection and storage are needed in the future.

In addition, we found that preterm colostrum and mature milk contain higher concentrations of PC than their term counterpart. PC is an important source of choline, along with SM, accounting for approximately 17% of the choline in HM [49]. Research has shown that choline is essential to fetal development [50,51]. The three- to fourfold higher choline concentration in fetal vs. term infant plasma corresponds to the fetus's higher growth rate and choline requirements [52,53]. Plasma choline, however, rapidly and prematurely decreases after preterm birth [52]. Low plasma choline levels may contribute to the impaired lean body mass growth of preterm infants. Recently, in a randomized controlled trial conducted by Bernhard W et al. [18], supplementation with 30 mg/kg/day additional choline increased plasma choline to near-fetal concentrations and improved DHA homeostasis in preterm infants. High concentrations of choline in human breast milk ensure the adequate supply of choline to the breastfed preterm infant, which help to preserve fetal concentrations of plasma choline in the perinatal period [18], thus playing a key role in tissue muscle accumulation, as required for the catch-up growth of premature infants after birth.

Conclusions

Preterm delivery interrupts the normal placental transfer and fetal accretion of choline, complex fatty acids, and phospholipids and fats that occur in the third trimester. Our findings offer useful information for the utilization of these critical constituents as nutritional, as well as functional, factors in infant formula, especially for EPT and VPT. Our metabolomic pathway analysis results provide novel insights into the mechanisms of human milk lipids' actions in neonatal development.

The vacancy of EPT colostrum samples is a substantial limitation to this study. Further explorations of HM composition in preterm infants will help in the more effective application of nutritional support strategies for preterm infants, especially EPT and VPT.

Abbreviations

GA: gestational age; VPT: very preterm; EPT: extremely preterm; MPT: moderate preterm; HM: human milk; TAG: triacylglycerol; PL: phospholipids; LC-MS/MS: liquid chromatography tandem–mass spectrometry; FM: formula milk; FT: full-term; PC: phosphatidylcholine; SM: sphingomyelin; PE: phosphatidylethanolamine; DAG: diacylglycerol; OPLS-DA: orthogonal partial least-squares discriminant analysis; VIP : variable importance in projection; FA: free fatty acid; FAHFA: fatty acid ester of hydroxyl fatty acid ; Acar: acylcarnitine; Cer/AP: ceramide alpha-hydroxy fatty acid-phytospingosine; Cer/AS: ceramide alpha-hydroxy fatty acid-sphingosine; DGTS: Diacylglyceryl trimethylhomoserine; LPE: lysophosphatidylethanolamine; MAG: monoacylglycerol ; GPI: glycosylphosphatidylinositol; MFGM: milk fat globule membrane; GLP-1: glucagon-like peptide 1; LC-PUFA: long-chain polyunsaturated fatty acids fatty acids; DHA: docosahexaenoic acid ; AA: arachidonic acid; GPL: glycerophospholipids; SL: sphingolipid.

Declarations

Ethics approval and consent to participate

The study was conducted in accordance with the Declaration of Helsinki and the protocol was approved by the Ethics Committee of the Children's Hospital of Fudan University (Children's Hospital of Fudan University Ethics Protocol 2019–087). Informed consent was obtained from all subjects involved in the study.

Consent for publication

Not applicable

Availability of data and materials

The dataset(s) supporting the conclusions of this article is(are) included within the article (and its additional file(s)).

Competing interests

The authors declare that they have no competing interests.

Funding

This research was funded by the Young Clinical Scientist Program of Fudan Academy of Pediatrics (grant no. EK112520180307).

Authors' contributions

PD and YCZ conceived and designed the study. CXL, YCZ, DYY collected the breast milk samples. PD and YCZ supervised the laboratory detection and bioinformatic analysis. YZ collected and analyzed the clinical data. PD interpreted the results and wrote the original draft. YCZ, CXL and YZ reviewed and edited the draft. PD acquired the funding. All authors read and approved the final manuscript.

Acknowledgments

The authors would like to acknowledge Dr. Chen-bo Ji from the Women's Hospital of Nanjing Medical University, Nanjing Maternity and Child Health Care Hospital (Nanjing, China) who kindly helped us organize the collection of full-term breast milk. We thank all of the mothers and infants who kindly donated their milk. We thank the assistance from Shanghai Biotree Biotech Co., Ltd.

References

1. Blencowe H, Cousens S, Chou D, Oestergaard M, Say L, Moller AB, et al. Born Too Soon: The global epidemiology of 15 million preterm births. Reprod Health. 2013;10.
2. Kong XY, Xu FD, Wu R, Wu H, Ju R, Zhao XL, et al. Neonatal mortality and morbidity among infants between 24 to 31 complete weeks: a multicenter survey in China from 2013 to 2014. Bmc Pediatr. 2016;16.
3. Boquien CY. Human Milk: An Ideal Food for Nutrition of Preterm Newborn. Front Pediatr. 2018;6:295.
4. Lewis ED, Richard C, Larsen BM, Field CJ. The Importance of Human Milk for Immunity in Preterm Infants. Clin Perinatol. 2017;44(1):23–47.
5. Corpeleijn WE, Kouwenhoven SMP, Paap MC, van Vliet I, Scheerder I, Muizer Y, et al. Intake of Own Mother's Milk during the First Days of Life Is Associated with Decreased Morbidity and Mortality in Very Low Birth Weight Infants during the First 60 Days of Life. Neonatology. 2012;102(4):276–81.
6. Lechner BE, Vohr BR. Neurodevelopmental Outcomes of Preterm Infants Fed Human Milk: A Systematic Review. Clin Perinatol. 2017;44(1):69–83.
7. Koletzko B. Human Milk Lipids. Ann Nutr Metab. 2016;69(Suppl 2):28–40.
8. Hernell O, Timby N, Domellof M, Lonnerdal B. Clinical Benefits of Milk Fat Globule Membranes for Infants and Children. J Pediatr. 2016;173(Suppl):60-5.
9. Alexandre-Gouabau MC, Moyon T, Cariou V, Antignac JP, Qannari EM, Croyal M, et al. Breast Milk Lipidome Is Associated with Early Growth Trajectory in Preterm Infants. Nutrients. 2018;10(2).
10. Jensen RG. The lipids in human milk. Prog Lipid Res. 1996;35(1):53–92.

11. Sun C, Wei W, Zou X, Huang J, Jin Q, Wang X. Evaluation of triacylglycerol composition in commercial infant formulas on the Chinese market: A comparative study based on fat source and stage. Food Chem. 2018;252:154–62.
12. Tu A, Ma Q, Bai H, Du Z. A comparative study of triacylglycerol composition in Chinese human milk within different lactation stages and imported infant formula by SFC coupled with Q-TOF-MS. Food Chem. 2017;221:555–67.
13. Jiang C, Ma B, Song S, Lai OM, Cheong LZ. Fingerprinting of Phospholipid Molecular Species from Human Milk and Infant Formula Using HILIC-ESI-IT-TOF-MS and Discriminatory Analysis by Principal Component Analysis. J Agric Food Chem. 2018;66(27):7131–8.
14. Zhu D, Hayman A, Kebede B, Stewart I, Chen G, Frew R. (31)P NMR-Based Phospholipid Fingerprinting of Powdered Infant Formula. J Agric Food Chem. 2019;67(36):10265–72.
15. George AD, Gay MCL, Trengove RD, Geddes DT. Human Milk Lipidomics: Current Techniques and Methodologies. Nutrients. 2018;10(9).
16. Sokol E, Ulven T, Faergeman NJ, Ejsing CS. Comprehensive and quantitative profiling of lipid species in human milk, cow milk and a phospholipid-enriched milk formula by GC and MS/MS(ALL). Eur J Lipid Sci Technol. 2015;117(6):751–9.
17. Hewelt-Belka W, Garwolinska D, Mlynarczyk M, Kot-Wasik A. Comparative Lipidomic Study of Human Milk from Different Lactation Stages and Milk Formulas. Nutrients. 2020;12(7).
18. Bernhard W, Bockmann K, Maas C, Mathes M, Hovelmann J, Shunova A, et al. Combined choline and DHA supplementation: a randomized controlled trial. Eur J Nutr. 2020;59(2):729–39.
19. Ingvordsen Lindahl IE, Artegoitia VM, Downey E, O'Mahony JA, O'Shea CA, Ryan CA, et al. Quantification of Human Milk Phospholipids: the Effect of Gestational and Lactational Age on Phospholipid Composition. Nutrients. 2019;11(2).
20. Xu L, Chen W, Wang X, Yu Z, Han S. Comparative Lipidomic Analyses Reveal Different Protections in Preterm and Term Breast Milk for Infants. Front Pediatr. 2020;8:590.
21. Chen Y, Ma Z, Shen X, Li L, Zhong J, Min LS, et al. Serum Lipidomics Profiling to Identify Biomarkers for Non-Small Cell Lung Cancer. Biomed Res Int. 2018;2018:5276240.
22. Chen Y, Ma Z, Zhong J, Li L, Min L, Xu L, et al. Simultaneous quantification of serum monounsaturated and polyunsaturated phosphatidylcholines as potential biomarkers for diagnosing non-small cell lung cancer. Sci Rep. 2018;8(1):7137.
23. Zhu T, Li S, Wang J, Liu C, Gao L, Zeng Y, et al. Induced sputum metabolomic profiles and oxidative stress are associated with chronic obstructive pulmonary disease (COPD) severity: potential use for predictive, preventive, and personalized medicine. EPMA J. 2020;11(4):645–59.
24. Deng J, Xia Z, Qiu D, Jiao X, Xiao B, Zhou W, et al. Nontarget metabolomics profiling of neuromyelitis optica spectrum disorder. Biomed Chromatogr. 2019;33(7):e4533.
25. XueKe G, Shuai Z, JunYu L, LiMin L, LiJuan Z, JinJie C. Lipidomics and RNA-Seq Study of Lipid Regulation in Aphis gossypii parasitized by Lysiphlebia japonica. Sci Rep. 2017;7(1):1364.
26. Uhl O, Hellmuth C, Demmelmair H, Zhou SJ, Makrides M, Prosser C, et al. Dietary Effects on Plasma Glycerophospholipids. J Pediatr Gastroenterol Nutr. 2015;61(3):367–72.
27. Uhl O, Glaser C, Demmelmair H, Koletzko B. Reversed phase LC/MS/MS method for targeted quantification of glycerophospholipid molecular species in plasma. J Chromatogr B Analyt Technol Biomed Life Sci. 2011;879(30):3556–64.
28. Hellmuth C, Uhl O, Segura-Moreno M, Demmelmair H, Koletzko B. Determination of acylglycerols from biological samples with chromatography-based methods. J Sep Sci. 2011;34(24):3470–83.
29. Hellmuth C, Weber M, Koletzko B, Peissner W. Nonesterified fatty acid determination for functional lipidomics: comprehensive ultrahigh performance liquid chromatography-tandem mass spectrometry quantitation, qualification, and parameter prediction. Anal Chem. 2012;84(3):1483–90.
30. Hellmuth C, Demmelmair H, Schmitt I, Peissner W, Bluher M, Koletzko B. Association between plasma nonesterified fatty acids species and adipose tissue fatty acid composition. PLoS One. 2013;8(10):e74927.
31. Rauschert S, Uhl O, Koletzko B, Kirchberg F, Mori TA, Huang RC, et al. Lipidomics Reveals Associations of Phospholipids With Obesity and Insulin Resistance in Young Adults. J Clin Endocrinol Metab. 2016;101(3):871–9.
32. Reinehr T, Wolters B, Knop C, Lass N, Hellmuth C, Harder U, et al. Changes in the serum metabolite profile in obese children with weight loss. Eur J Nutr. 2015;54(2):173–81.
33. Rzehak P, Hellmuth C, Uhl O, Kirchberg FF, Peissner W, Harder U, et al. Rapid growth and childhood obesity are strongly associated with lysoPC(14:0). Ann Nutr Metab. 2014;64(3–4):294–303.
34. Murase T, Mizuno T, Omachi T, Onizawa K, Komine Y, Kondo H, et al. Dietary diacylglycerol suppresses high fat and high sucrose diet-induced body fat accumulation in C57BL/6J mice. J Lipid Res. 2001;42(3):372–8.

35. Kamphuis MM, Mela DJ, Westerterp-Plantenga MS. Diacylglycerols affect substrate oxidation and appetite in humans. Am J Clin Nutr. 2003;77(5):1133–9.
36. Yore MM, Syed I, Moraes-Vieira PM, Zhang T, Herman MA, Homan EA, et al. Discovery of a class of endogenous mammalian lipids with anti-diabetic and anti-inflammatory effects. Cell. 2014;159(2):318–32.
37. Kuda O, Brezinova M, Rombaldova M, Slavikova B, Posta M, Beier P, et al. Docosahexaenoic Acid-Derived Fatty Acid Esters of Hydroxy Fatty Acids (FAHFAs) With Anti-inflammatory Properties. Diabetes. 2016;65(9):2580–90.
38. Brejchova K, Balas L, Paluchova V, Brezinova M, Durand T, Kuda O. Understanding FAHFAs: From structure to metabolic regulation. Prog Lipid Res. 2020;79:101053.
39. Balas L, Bertrand-Michel J, Viars F, Faugere J, Lefort C, Caspar-Bauguil S, et al. Regiocontrolled syntheses of FAHFAs and LC-MS/MS differentiation of regioisomers. Org Biomol Chem. 2016;14(38):9012–20.
40. Lee J, Moraes-Vieira PM, Castoldi A, Aryal P, Yee EU, Vickers C, et al. Branched Fatty Acid Esters of Hydroxy Fatty Acids (FAHFAs) Protect against Colitis by Regulating Gut Innate and Adaptive Immune Responses. J Biol Chem. 2016;291(42):22207–17.
41. Brezinova M, Kuda O, Hansikova J, Rombaldova M, Balas L, Bardova K, et al. Levels of palmitic acid ester of hydroxystearic acid (PAHSA) are reduced in the breast milk of obese mothers. Biochim Biophys Acta Mol Cell Biol Lipids. 2018;1863(2):126–31.
42. Gallier S, Gragson D, Cabral C, Jimenez-Flores R, Everett DW. Composition and fatty acid distribution of bovine milk phospholipids from processed milk products. J Agric Food Chem. 2010;58(19):10503–11.
43. Saele O, Rod KEL, Quinlivan VH, Li S, Farber SA. A novel system to quantify intestinal lipid digestion and transport. Biochim Biophys Acta Mol Cell Biol Lipids. 2018;1863(9):948–57.
44. Wang L, Shimizu Y, Kaneko S, Hanaka S, Abe T, Shimasaki H, et al. Comparison of the fatty acid composition of total lipids and phospholipids in breast milk from Japanese women. Pediatr Int. 2000;42(1):14–20.
45. Moukarzel S, Dyer RA, Keller BO, Elango R, Innis SM. Human Milk Plasmalogens Are Highly Enriched in Long-Chain PUFAs. J Nutr. 2016;146(11):2412–7.
46. Maas C, Franz AR, Shunova A, Mathes M, Bleeker C, Poets CF, et al. Choline and polyunsaturated fatty acids in preterm infants' maternal milk. Eur J Nutr. 2017;56(4):1733–42.
47. Gonzalez HF, Visentin S. Nutrients and neurodevelopment: lipids. Arch Argent Pediatr. 2016;114(5):472–6.
48. Campoy C, Escolano-Margarit MV, Anjos T, Szajewska H, Uauy R. Omega 3 fatty acids on child growth, visual acuity and neurodevelopment. Br J Nutr. 2012;107(Suppl 2):85–106.
49. Cilla A, Diego Quintaes K, Barbera R, Alegria A. Phospholipids in Human Milk and Infant Formulas: Benefits and Needs for Correct Infant Nutrition. Crit Rev Food Sci Nutr. 2016;56(11):1880–92.
50. Radziejewska A, Chmurzynska A. Folate and choline absorption and uptake: Their role in fetal development. Biochimie. 2019;158:10–9.
51. Zeisel SH. Choline: critical role during fetal development and dietary requirements in adults. Annu Rev Nutr. 2006;26:229–50.
52. Bernhard W, Raith M, Kunze R, Koch V, Heni M, Maas C, et al. Choline concentrations are lower in postnatal plasma of preterm infants than in cord plasma. Eur J Nutr. 2015;54(5):733–41.
53. Voigt M, Rochow N, Straube S, Briese V, Olbertz D, Jorch G. Birth weight percentile charts based on daily measurements for very preterm male and female infants at the age of 154–223 days. J Perinat Med. 2010;38(3):289–95.

Tables

Table 1
Baseline characteristics of the infants and breastfeeding mothers

	Colostrum (< 5 postpartum days)				Mature milk (4 weeks postpartum)				
	VPT (n = 20)	MPT (n = 20)	FT (n = 30)	P-value	EPT (n = 11)	VPT (n = 23)	MPT (n = 21)	FT (n = 25)	P-value
Gestational age(mean (SD))	30.13(1.08)	34.14(1.25)	39.10(1.11)	< 0.001	26.49(1.16)	29.76(0.89)	32.78(0.67)	38.77(0.92)	< 0.001
Range (weeks)	28.43–31.86	32.29–36.43	37.71–41.29	< 0.001	24.00-27.86	28.14–31.71	32.00-34.14	37.00-41.57	< 0.001
Birth weight(mean (SD))	1511(273)	1916(322)	3370(339)	0.544	973(210)	1380(170)	1545(335)	3322(314)	< 0.05
Range (g)	1050–1920	1150–2445	2600–4251	0.631	800–1420	1080–1730	910–2300	2557–4110	0.891
Male(n (%))	13(65%)	12(60%)	17(57%)	0.738	6(55%)	15(65%)	8(38%)	13(52%)	0.522
Maternal age(mean (SD))	31(4)	29(4)	29(4)	< 0.001	33(5)	32(4)	33(4)	31(5)	< 0.001
Range (years)	25–37	23–38	23–38		28–45	25–40	24–40	21–42	
Maternal BMI at birth(mean (SD))	22.22(4.11)	22.01(4.19)	21.9(3.74)		22.67(4.45)	21.55(3.28)	22.97(4.09)	22.11(4.44)	
Range (kg/m^2)	17.72–31.13	17.15–29.98	18.00-28.03		18.15–28.03	18.01–31.13	17.78–30.06	17.50-31.11	
Cesarean section (%)	95.60%	87.33%	33.44%		99.91%	97.44%	87.47%	36.35%	

EPT: extremely preterm; VPT: very preterm; MPT: moderately preterm; FT: full-term.

Table 2
The top 10 most notably upregulated lipids in VPT colostrum as compared with FT counterpart

Name	VPT	FT	VIP	*P*-value
Upregulated				
PE(18:1/22:1)	0.02666	0.01349	1.58808	1.37E-07
PE(18:1/20:1)	0.14709	0.0775	1.53485	1.19E-06
DAG(12:0/22:5)	0.02751	0.01009	1.33663	1.19E-06
ACar(18:3)	0.00611	0.00229	1.09655	1.24E-06
DAG(16:0/22:6)	0.06557	0.02807	1.21894	2.47E-06
PE(14:1/26:4)	0.06333	0.0384	1.15569	3.11E-06
PE(16:0/16:0)	0.0386	0.02178	1.05767	6.90E-06
DAG(14:1/18:1)	0.4422	0.08157	1.29495	8.06E-06
FAHFA(16:2/26:4)	2.18617	0.39658	1.5826	8.59E-06
HexCer/NS(d14:3/19:1)	0.01103	0.00453	1.57603	9.98E-06

VPT: very preterm; FT: full-term; VIP: variable importance in projection of the OPLS-DA model

Table 3
The top 10 most notably upregulated lipids in EPT mature milk as compared with FT counterpart

Name	EPT	FT	VIP	*P*-value
Upregulated				
FA(18:1)	0.70866	0.51798	1.64705	5.23E-08
FA(16:2)	0.70769	0.17423	1.87897	6.32E-08
GlcADG(12:0/17:2)	0.02729	0.00664	1.74735	2.48E-07
FAHFA(16:1/22:4)	0.007	0.00207	1.67575	1.51E-06
FA(17:3)	0.02023	0.00502	1.82093	2.24E-06
DAG(18:0/20:4)	0.0167	0.00257	2.48566	3.90E-06
FAHFA(22:3/22:4)	0.01687	0.00354	1.69943	6.28E-06
FA(19:2)	0.10731	0.03116	1.76184	2.96E-05
FAHFA(2:0/17:2)	0.12484	0.04769	1.68875	0.000101
FAHFA(20:2/20:1)	0.01762	0.00357	1.65397	0.000124

EPT: extremely preterm; FT: full-term; VIP: variable importance in projection of the OPLS-DA model

Table 4
The top 10 most notably upregulated lipids in VPT mature milk as compared with FT counterpart

Name	VPT	FT	VIP	*P*-value
Upregulated				
GlcADG(12:0/17:2)	0.02755	0.00664	1.90786	7.50E-09
FA(16:2)	0.60226	0.17423	1.93359	4.25E-08
FAHFA(18:2/14:1)	0.00846	0.00097	1.89332	4.59E-07
Cer/AS(d19:3/16:2)	0.10244	0.0128	1.81358	7.13E-07
FAHFA(16:1/22:4)	0.00616	0.00207	1.79913	8.28E-07
FAHFA(20:3/22:5)	0.05209	0.01026	1.93091	1.35E-06
FA(17:3)	0.01654	0.00502	1.91319	1.4E-06
FA(18:1)	0.66552	0.51798	1.44257	1.77E-06
FAHFA(12:0/18:2)	0.05398	0.00845	1.82852	1.91E-06
FAHFA(18:1/18:2)	0.71503	0.13136	1.80522	1.97E-06

VPT: very preterm; FT: full-term; VIP: variable importance in projection of the OPLS-DA model

Figures

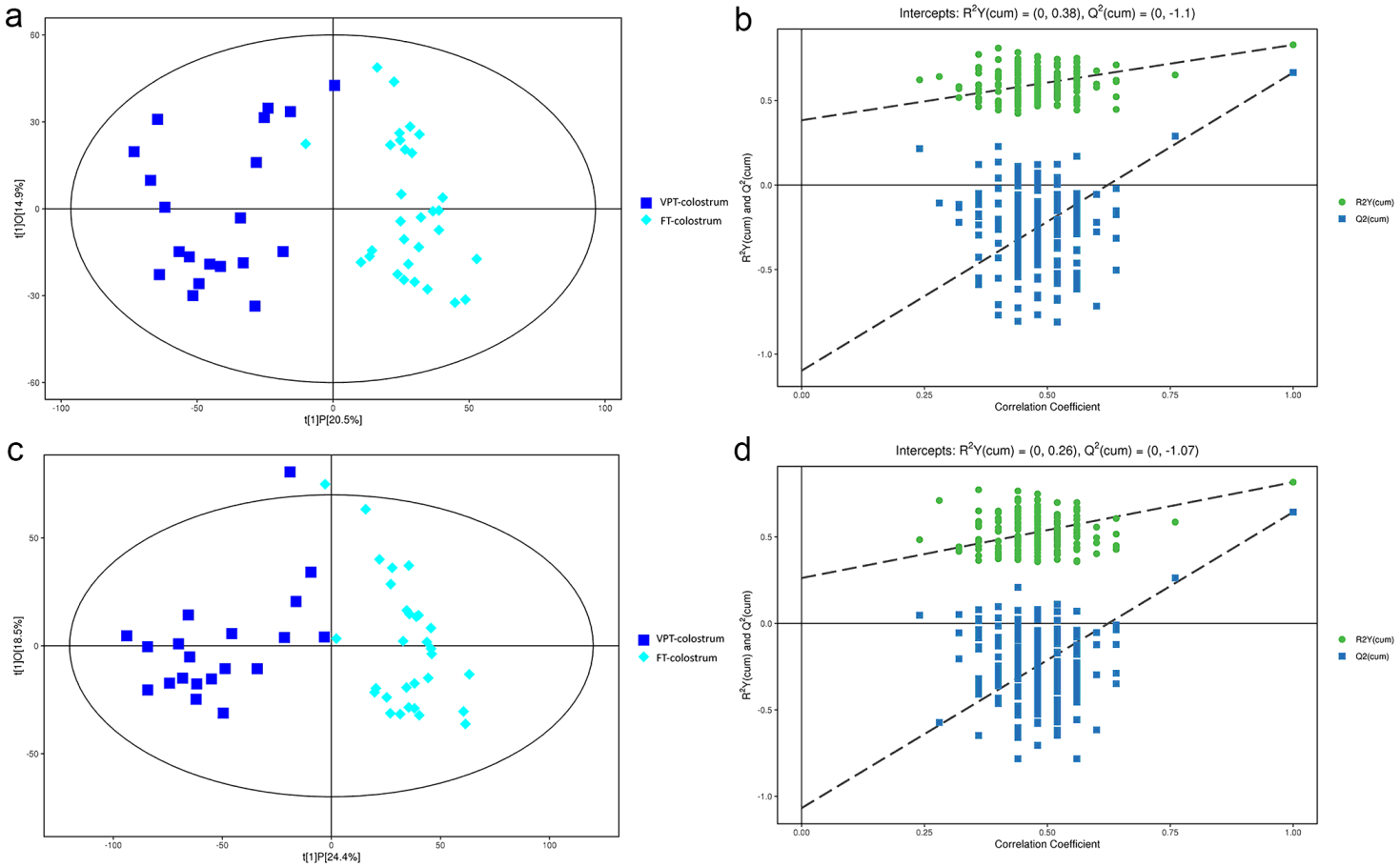

Figure 1

Score scatter plot and permutation test of OPLS-DA model between VPT colostrum and FT colostrum. (a) Score plots were obtained in the negative ionization mode. X-t[1]P represents the predicted principal component score of the first principal component, showing the difference between the sample groups. Y-t[1]O represents the score of the orthogonal principal component, showing the difference within the sample group. Each scatter represents a sample, and the shape and color of the scatter indicate different experimental groups. (b) Permutation tests were obtained in the negative ionization mode. The X axis and Y axis represent the correlation coefficient and value of R2Y and Q2, respectively. (c) Score plots were obtained in the positive ionization mode. (d) Permutation tests were carried out in the positive ionization mode. OPLS-DA, orthogonal partial least-squares discriminant analysis.

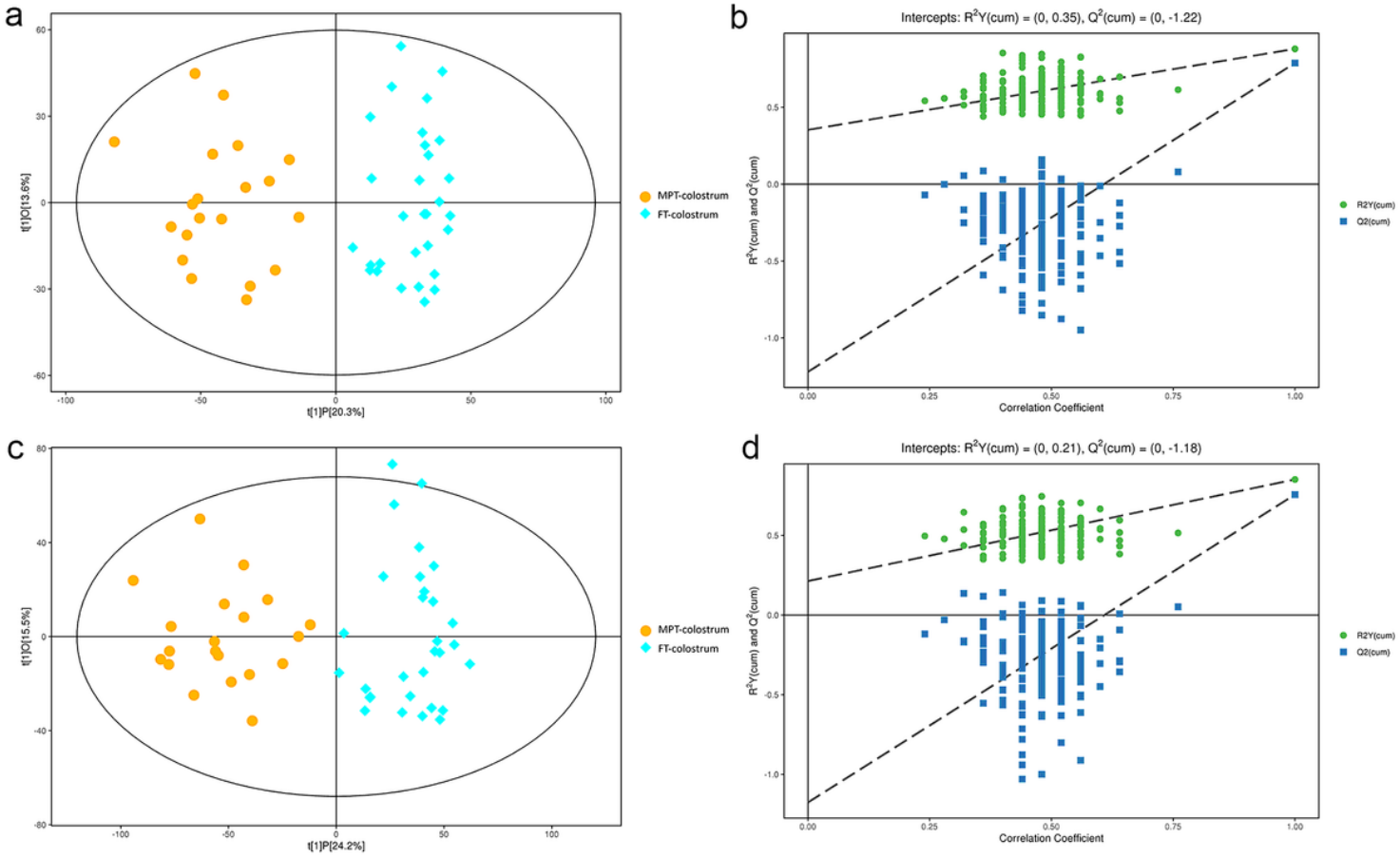

Figure 2

Score scatter plot and permutation test of OPLS-DA model between MPT colostrum and FT colostrum. (a) Score plots were obtained in the negative ionization mode. X-t[1]P represents the predicted principal component score of the first principal component, showing the difference between the sample groups. Y-t[1]O represents the score of the orthogonal principal component, showing the difference within the sample group. Each scatter represents a sample, and the shape and color of the scatter indicate different experimental groups. (b) Permutation tests were carried out in the negative ionization mode. The X axis and Y axis represent the correlation coefficient and the value of R2Y and Q2, respectively. (c) Score plots were obtained in the positive ionization mode. (d) Permutation tests were carried out in the positive ionization mode. OPLS-DA, orthogonal partial least-squares discriminant analysis.

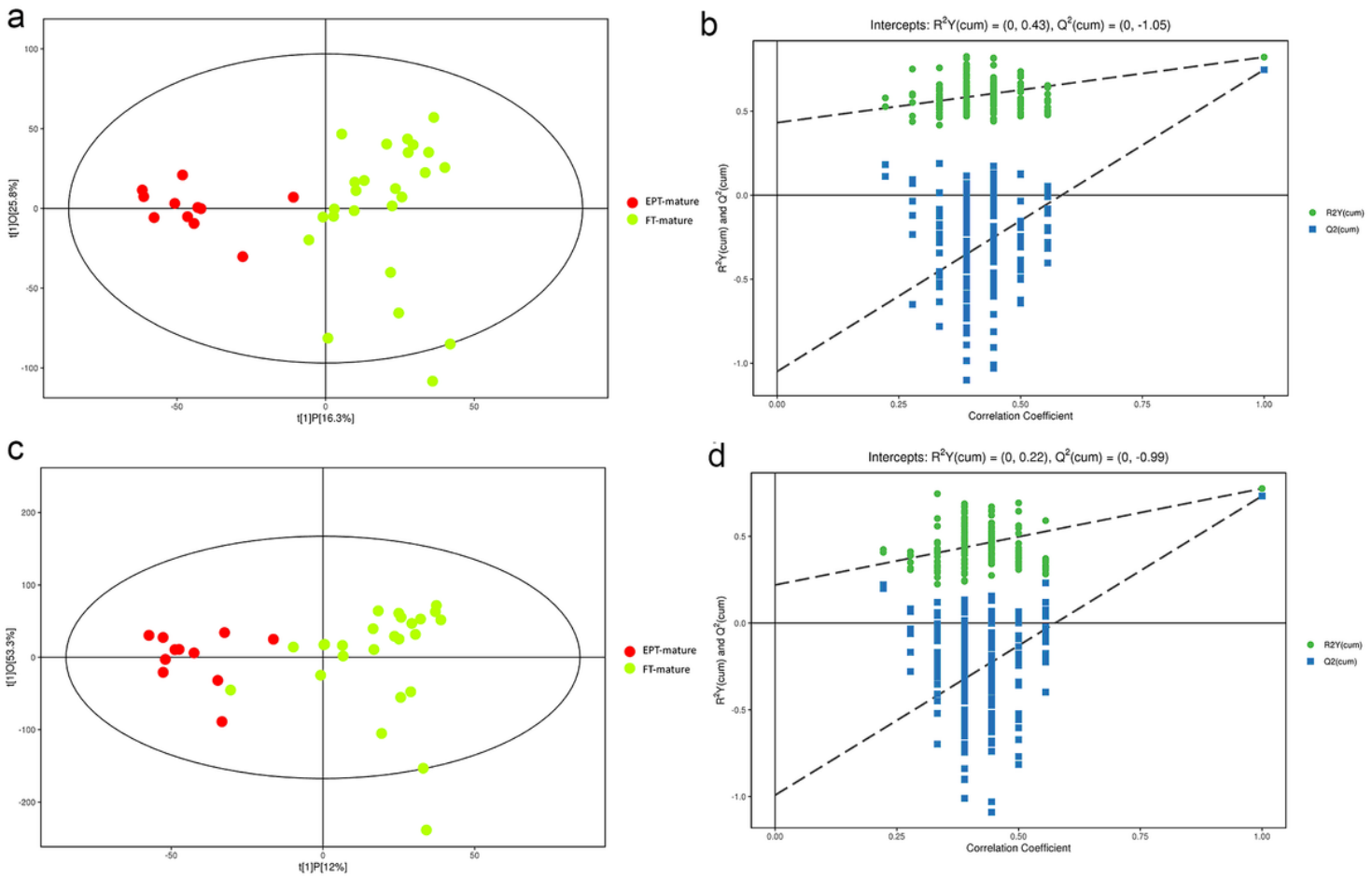

Figure 3

Score scatter plot and permutation test of the OPLS-DA model between EPT mature and FT mature. (a) Score plots were obtained in the negative ionization mode. X-t[1]P represents the predicted principal component score of the first principal component, showing the difference between the sample groups. Y-t[1]O represents the score of the orthogonal principal component, showing the difference within the sample group. Each scatter represents a sample, and the shape and color of the scatter indicate different experimental groups. (b) Permutation tests were obtained in the negative ionization mode. The X axis and Y axis represent the correlation coefficient and the value of R2Y and Q2, respectively. (c) Score plots were obtained in the positive ionization mode. (d) Permutation tests were carried out in the positive ionization mode. OPLS-DA, orthogonal partial least-squares discriminant analysis.

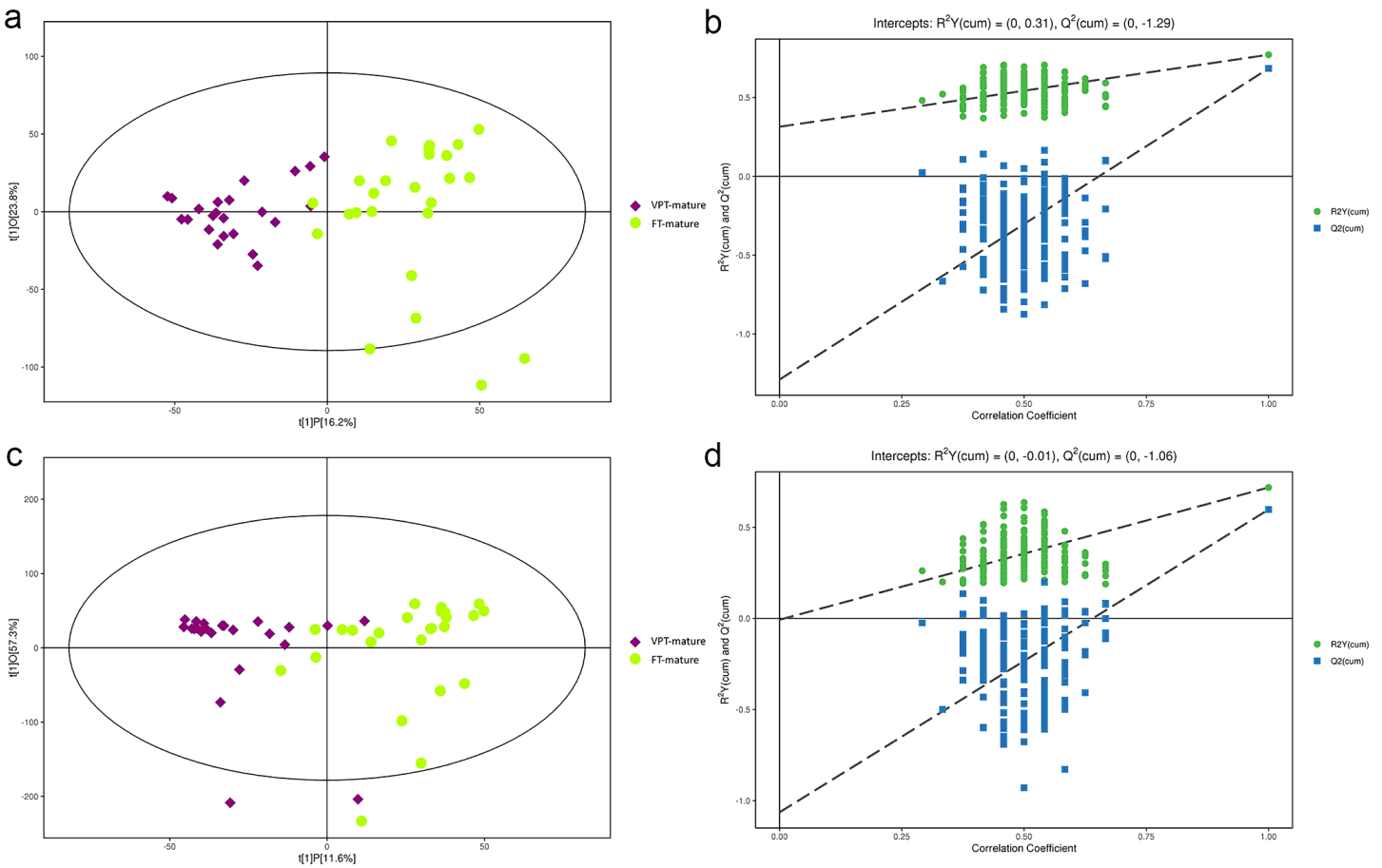

Figure 4

Score scatter plot and permutation test of the OPLS-DA model between VPT mature and FT mature. (a) Score plots were obtained in the negative ionization mode. X-t[1]P represents the predicted principal component score of the first principal component, showing the difference between the sample groups. Y-t[1]O represents the score of the orthogonal principal component, showing the difference within the sample group. Each scatter represents a sample, and the shape and color of the scatter indicate different experimental groups. (b) Permutation tests were obtained in the negative ionization mode. The X axis and Y axis represent the correlation coefficient and the value of R2Y and Q2, respectively. (c) Score plots were obtained in the positive ionization mode. (d) Permutation tests were carried out in the positive ionization mode. OPLS-DA, orthogonal partial least-squares discriminant analysis.

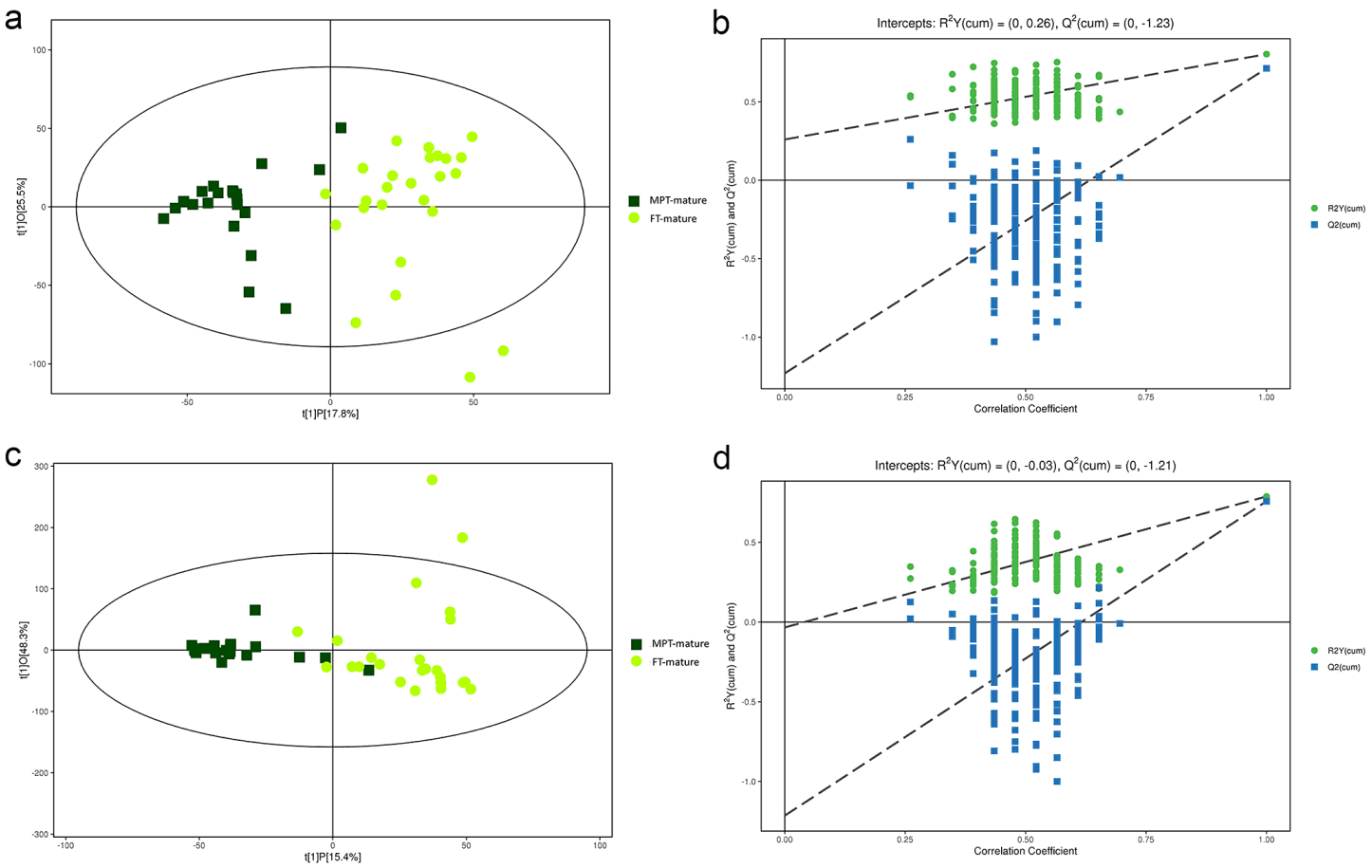

Figure 5

Score scatter plot and permutation test of OPLS-DA model between MPT mature and FT mature. (a) Score plots were obtained in the negative ionization mode. X-t[1]P represents the predicted principal component score of the first principal component, showing the difference between the sample groups. Y-t[1]O represents the score of the orthogonal principal component, showing the difference within the sample group. Each scatter represents a sample, and the shape and color of the scatter indicate different experimental groups. (b) Permutation tests were carried out in the negative ionization mode. The X axis and Y axis represent the correlation coefficient and the value of R2Y and Q2, respectively. (c) Score plots were obtained in the positive ionization mode. (d) Permutation tests were carried out in the positive ionization mode. OPLS-DA, orthogonal partial least-squares discriminant analysis.

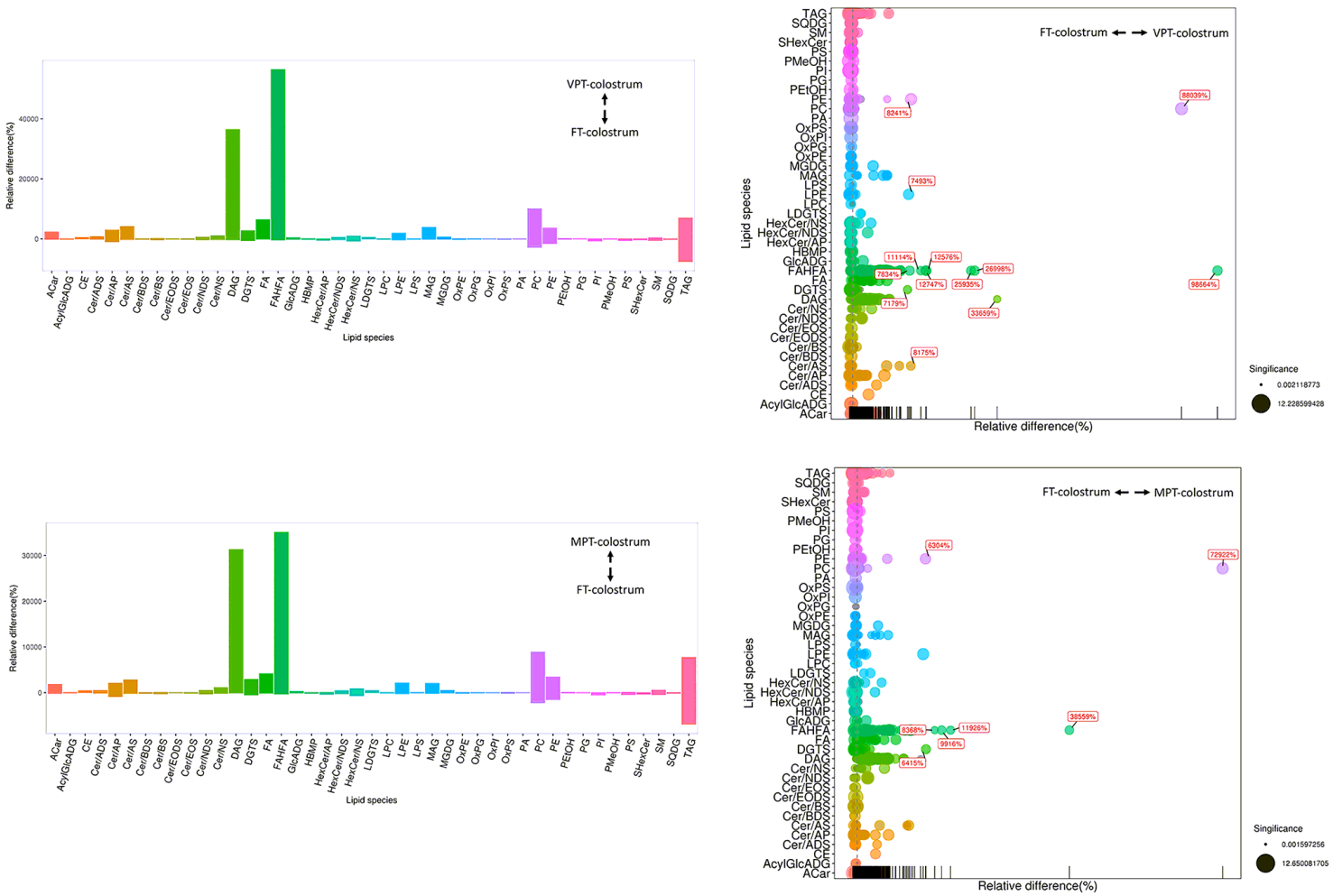

Figure 6

Bar plot and bubble plot of lipidomics analysis in the colostrum. In the bar plot, the X axis represents the classification information of lipids, and the Y axis represents the relative change percentage of each lipid's content. If the relative percentage change in content is zero, the substance is present at the same level in both groups. The relative percentage change was positive, indicating that the lipid content was higher in the preterm group. The percentage of relative content change was negative, indicating that the lipid content was higher in the term group. In the bubble plot, each point represents a substance. The size of the point represents the P-value of the corresponding Student's t-test (negative number of logarithms based on 10); the larger the point, the smaller the P-value. Gray points represent non-significant differences with P-values no less than 0.05, and colored points represent significant differences with P-values less than 0.05 (different colors according to lipid classification). The X axis represents the relative change percentage of the content of each substance (the relative change percentage of the substance with the greatest change is directly marked on its point, and the relative change percentages of the other substances are shown in the corresponding abscissa scale). The Y axis depicts the classification information of lipids. If the relative change percentage of the content is zero, the contents in the two groups were the same. If the relative change percentage of the content is positive, the content of the substance in the preterm group was higher. If the relative change percentage of the content is negative, the content of the substance in the term group was higher. The black line at the bottom shows the distribution density of lipids (each line represents a substance).

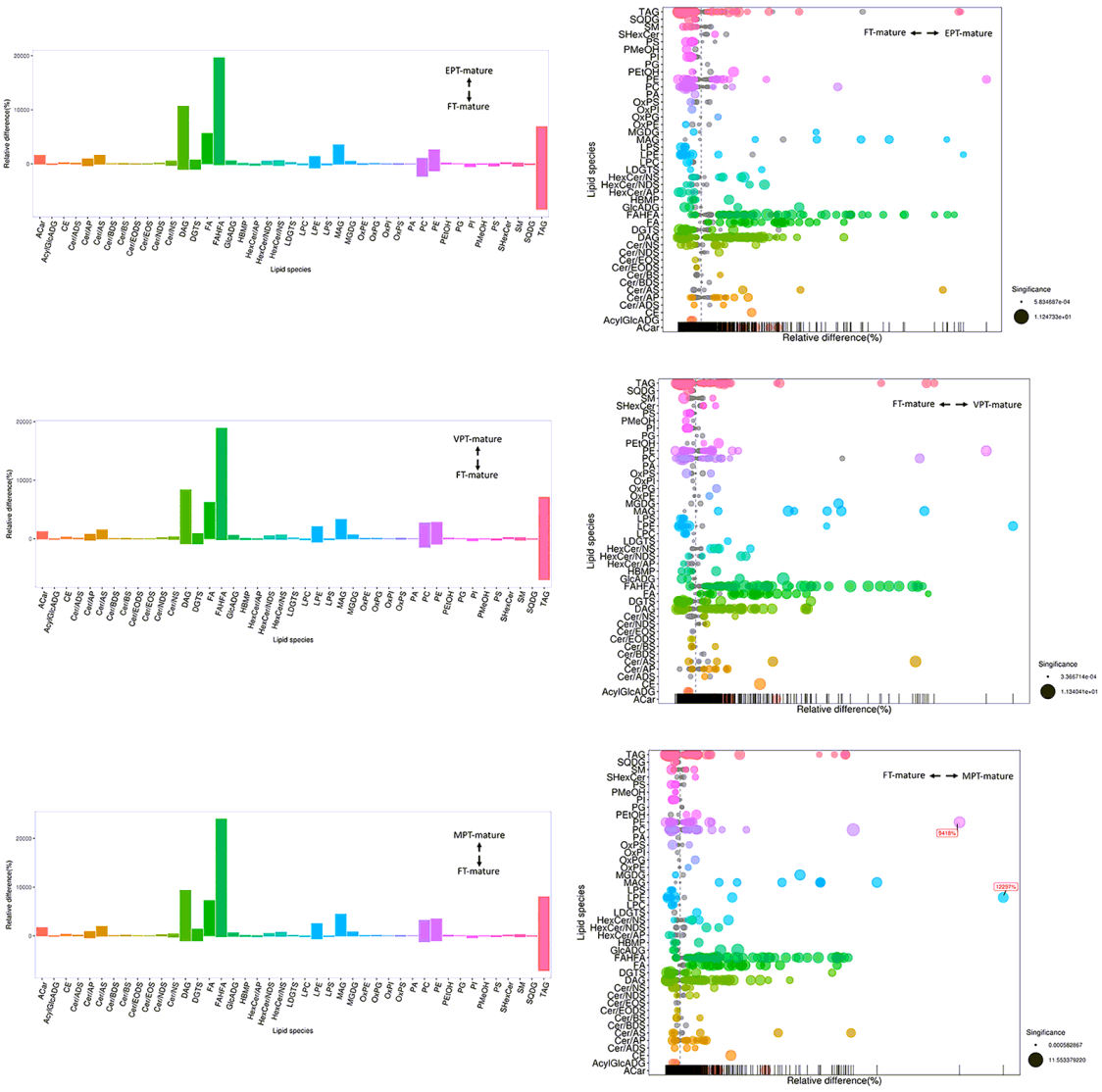

Figure 7

Bar plot and bubble plot of lipidomics analysis in mature milk. In the bar plot, the X axis represents the classification information of lipids, and the Y axis represents the relative change percentage of each lipid's content. If the relative percentage change in content is zero, the substance is present at the same level in both groups. The relative percentage change was positive, indicating that the lipid content was higher in the preterm group. The percentage of relative content change was negative, indicating that the lipid content was higher in the term group. In the bubble plot, each point represents a substance. The size of the point represents the P-value of the corresponding Student's t-test (negative number of logarithms based on 10), and the larger the point, the smaller the P-value. Gray points represent non-significant differences with P-values no less than 0.05, and colored points represent significant differences with P-values less than 0.05 (different colors according to lipid classification). The X axis represents the relative change percentage of the content of each substance (the relative change percentage of the substance with the greatest change is directly marked on its point, and the relative change percentages of the other substances are shown in the corresponding abscissa scale). The Y axis represents the classification information of the lipids. The relative change percentage of the content was zero, indicating that the contents of the substances in the two groups were the same. If the relative change percentage of the content is positive, the content of the substance in the preterm group was higher. If the relative change percentage of the content is negative, the content of the substance in the term group was higher. The black line at the bottom shows the distribution density of the lipids (each line represents a substance).

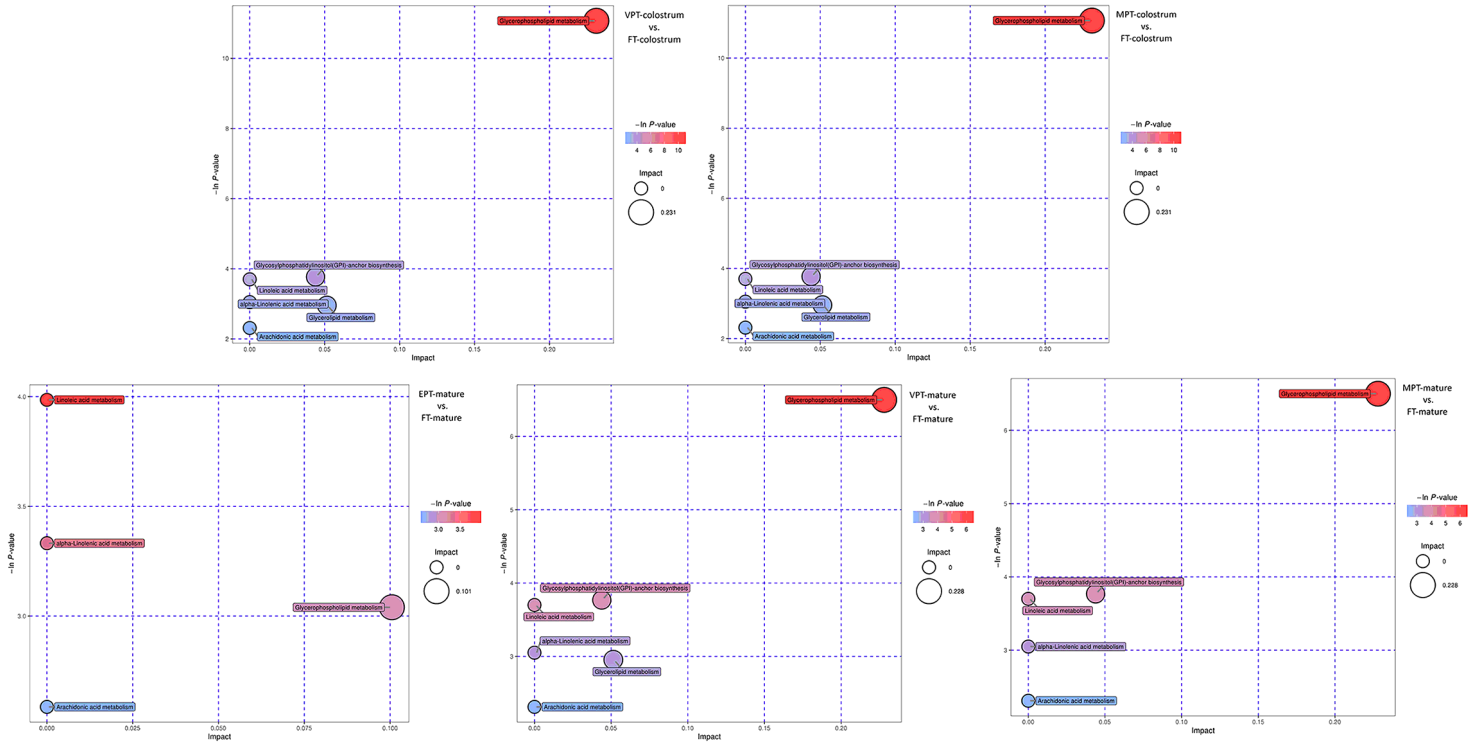

Figure 8

Pathway analysis of the significantly different lipids performed via MetaboAnalyst. The X axis represents the impact value of the metabolic pathway topology analysis. The Y axis represents the transformation of the original P-value (-ln(p)), calculated via enrichment analysis.

Supplementary Files

This is a list of supplementary files associated with this preprint. Click to download.

- FigureS1heatmapVPTFTcolostrumneg.pdf
- FigureS2heatmapVPTFTcolostrumpos.pdf
- FigureS3heatmapMPTFTcolostrumneg.pdf
- FigureS4heatmapMPTFTcolostrumpos.pdf
- FigureS5heatmapEPTFTmaturemilkneg.pdf
- FigureS6heatmapEPTFTmaturemilkpos.pdf
- FigureS7heatmapVPTFTmaturemilkneg.pdf
- FigureS8heatmapVPTFTmaturemilkpos.pdf
- FigureS9heatmapMPTFTmaturemilkneg.pdf
- FigureS10heatmapMPTFTmaturemilkpos.pdf
- TableS1NEGDifferentiallyExpressedMetabolites.xlsx
- TableS2POSDifferentiallyExpressedMetabolites.xlsx
- TableS3Top10lipidsincolostrumneg.docx
- TableS4Top10lipidsincolostrumpos.docx
- TableS5Top10lipidsinmaturemilkneg.docx
- TableS6Top10lipidsinmaturemilkpos.docx